Fig S1 Related to Figure 2

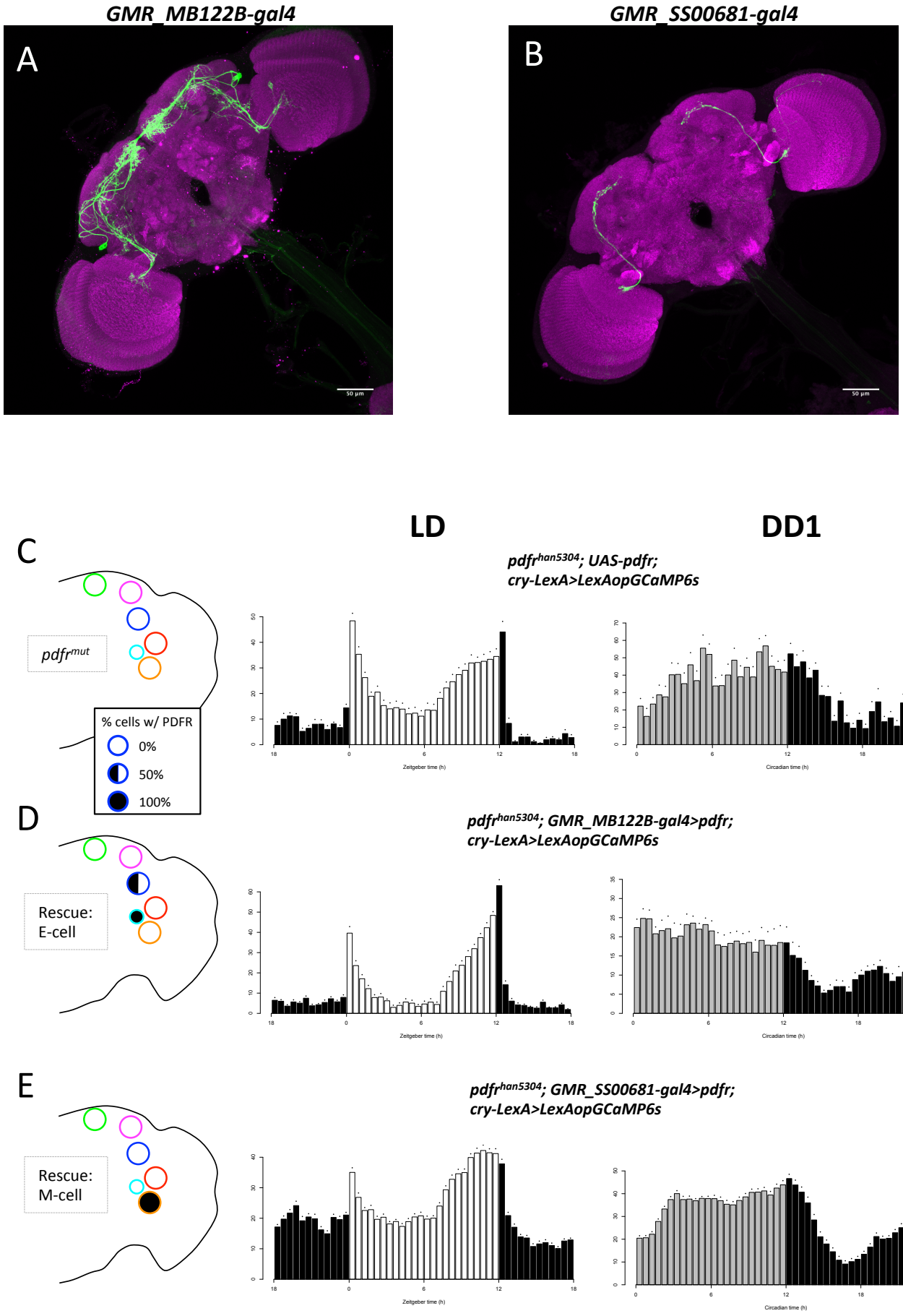

Figure S1. Restoring PDFR in E pacemakers partially rescued the evening behavioral phase in *pdfr* mutants. Related to Figure 2.

(A-B) The expression patterns of (A) MB122B-GAL4 and (B) SS00681-GAL4. The maximum intensity projections of 20x confocal stacks; the reference pattern is anti-Brp and the split-GAL4 pattern was visualized using a membrane targeted marker
(pJFRC225-5XUAS-IVS-myr::smGFP-FLAG). More detailed characterization of these lines will be presented in: H. Dionne, G. Rubin and A. Nern (in preparation).

(C-E) Average locomotor activity in the same genotypes which are used for imaging in Figure 2 B-D under LD cycles (left) and in first day under DD (right); also see Table S1. Restoring PDFR in M pacemakers did not provide such rescue. These results confirm previously published work by Lear et al. (2009) and by Im and Taghert (2010).

Fig S2. Related to Figure 4

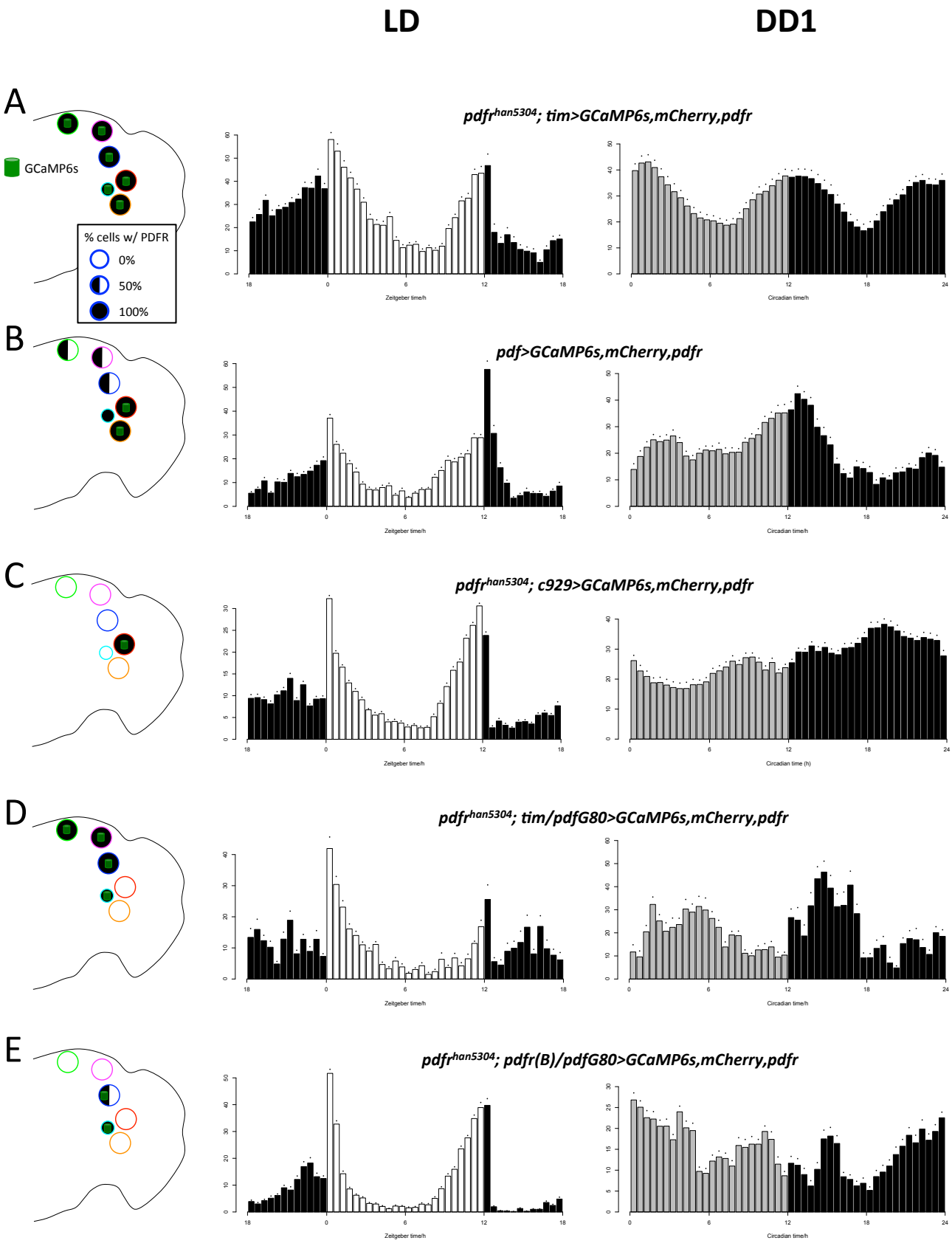

Figure S2. Behavioral patterns resulting from PDFR gain-of-function experiments. Related to Figure 4.

(A-E) Average locomotor activity under LD cycles (left) and in first day under DD (right) in in the same genotypes which were used for imaging in Figure 4 A-E (also see Table S1).

Fig S3 Related to Figure 5

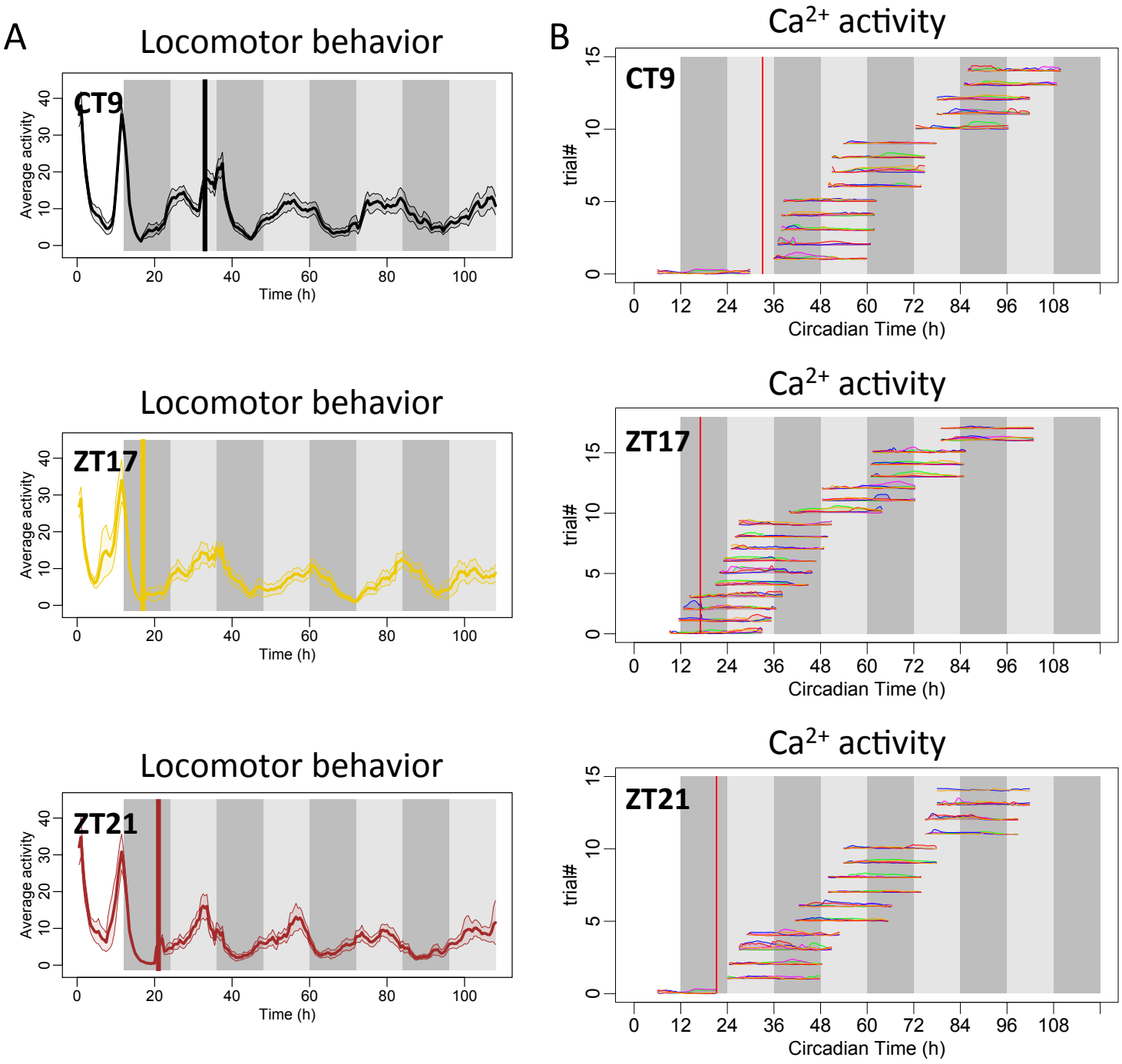

Figure S3. Behavior and Ca^{2+} activity phase-shifts by light pulses. Related to Figure 5.
(A) Average locomotor activity in the three days following 15 min light pulses delivered either in the dead zone (CT9), or in the phase-delay zone (ZT17), or in the phase-advance zone (ZT21). Bars indicate the time of light pulses. (n= 16 flies).
(B) Ca^{2+} activity traces of light pulse experiments. Each line represents a single imaging episode measuring 24 h Ca^{2+} transients in the different pacemaker groups in one fly. Group-specific traces were then tiled and averaged to synthesize the three-day patterns in Figure 5A. Red bars indicate the time of light pulses.

Fig S4. Related to Figure 5

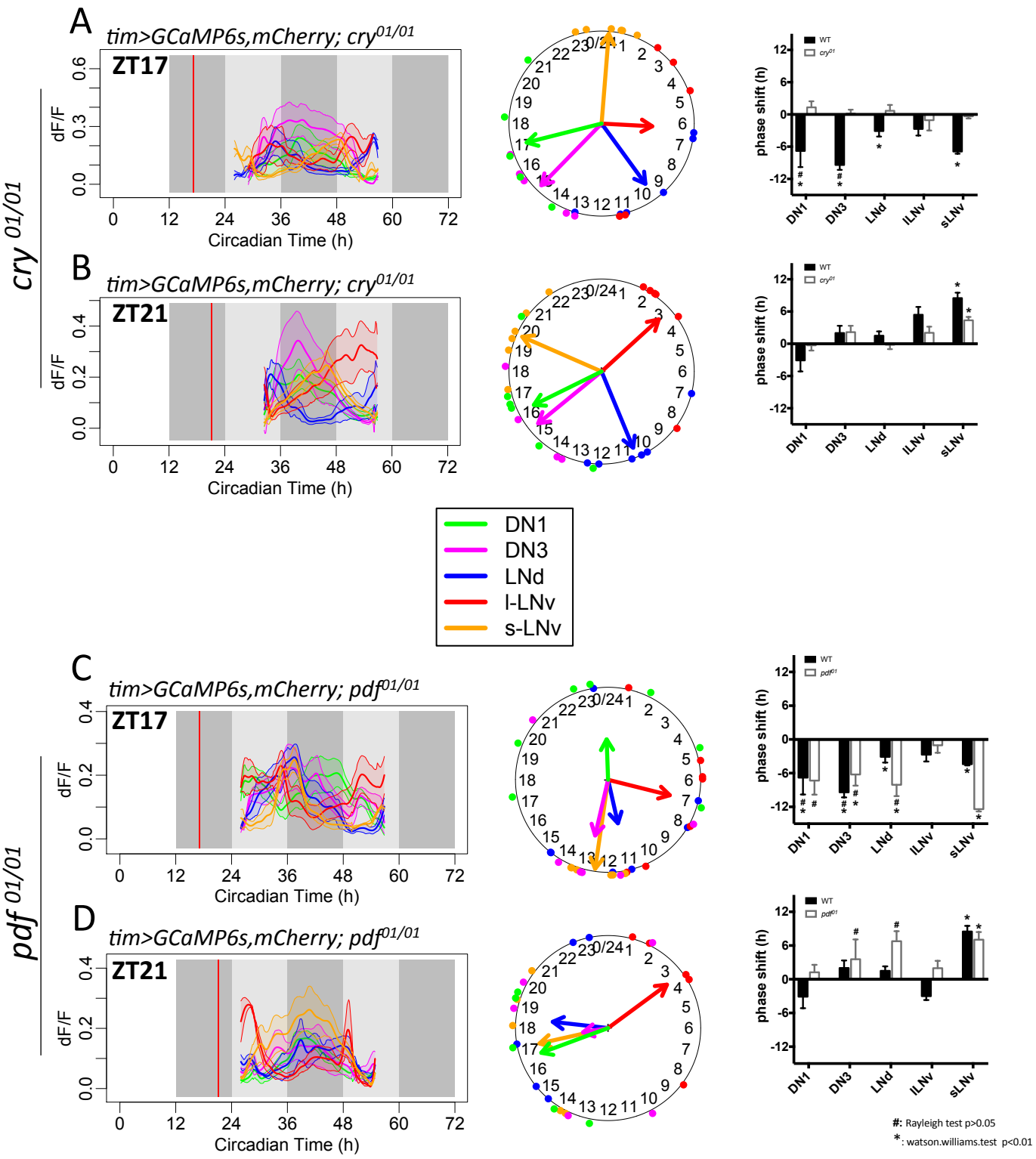

Figure S4. Light-induced Ca^{2+} phase-shifts require CRY and PDF. Related to Figure 5.
(A-B) Measurements of Ca^{2+} phase-shifts in the five major pacemaker groups in *cry*^{01} mutants *in vivo*, during the first day after light pulses: (A) in the phase-delay zone (ZT17; n = 6 flies) and (B) in the phase-advance zone (ZT21; n = 6 flies). Left, Ca^{2+} transients. Middle, Ca^{2+} phase distributions. Right, Ca^{2+} phase shifts by light pulses in WT controls (filled bars) and *cry*^{01} mutants (empty bars) compared to unstimulated WT controls and *cry*^{01} mutants respectively. Hashes (#) denote those groups losing coherence of Ca^{2+} activity ($p>0.05$: Rayleigh test). Asterisks denote those groups with significant phase-shifts ($p<0.01$: Watson-Williams test).
(C-D) Measurements of Ca^{2+} phase-shifts in the five major pacemaker groups *in vivo* in *pdf*^{01} mutants in the first day after light pulses (C) in the phase-delay zone (ZT17; n = 7 flies) and (D) in the phase-advance zone (ZT21; n = 5 flies).

Fig S5. Related to Figure 6

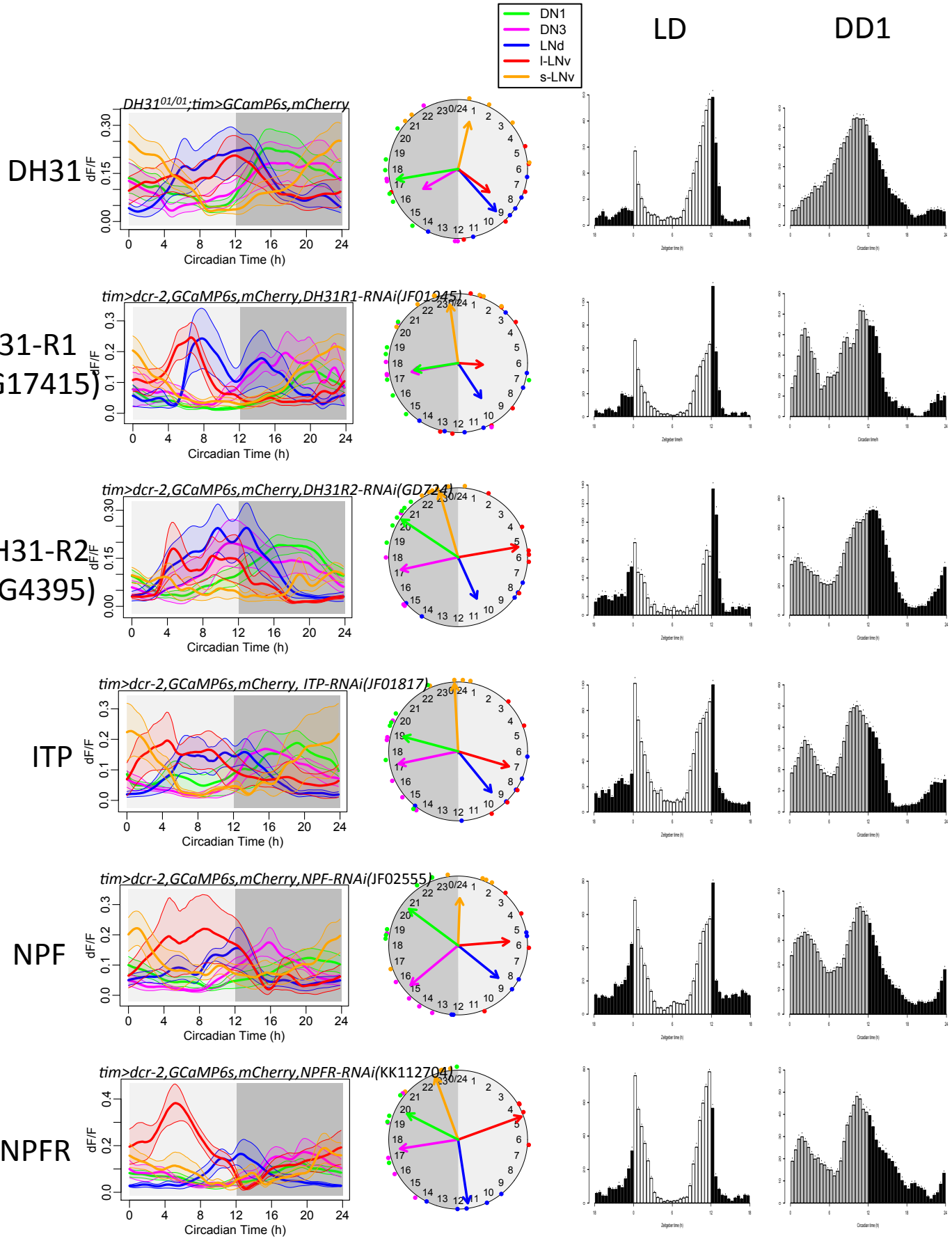

Figure S5. A screen for neuropeptides and cognate receptors that contribute to wild type patterns of Ca^{2+} rhythms. Related to Figure 6.

(Left) Daily Ca^{2+} activity patterns of the five major pacemaker groups under DD in flies with neuropeptide mutants or pan-pacemaker RNAi knockdown of neuropeptides or receptors. Left, average Ca^{2+} transients. Right, Ca^{2+} phase distributions. (DH31: n = 6 flies; DH31R1: n = 8 flies; DH31R2: n = 7 flies; ITP: n = 6 flies; NPF: n = 6 flies; NPFR: n = 5 flies)

(Right) Average locomotor activity under LD cycles and in first day under DD (DD1) in genotypes that were screened in the left panel (also see Table S1). The absence of a morning activity in *dh31*^{01} homozygotes has previously been ascribed to an unrelated genetic background effect (Kunst et al., 2014).

Fig S6. Related to Figure 6

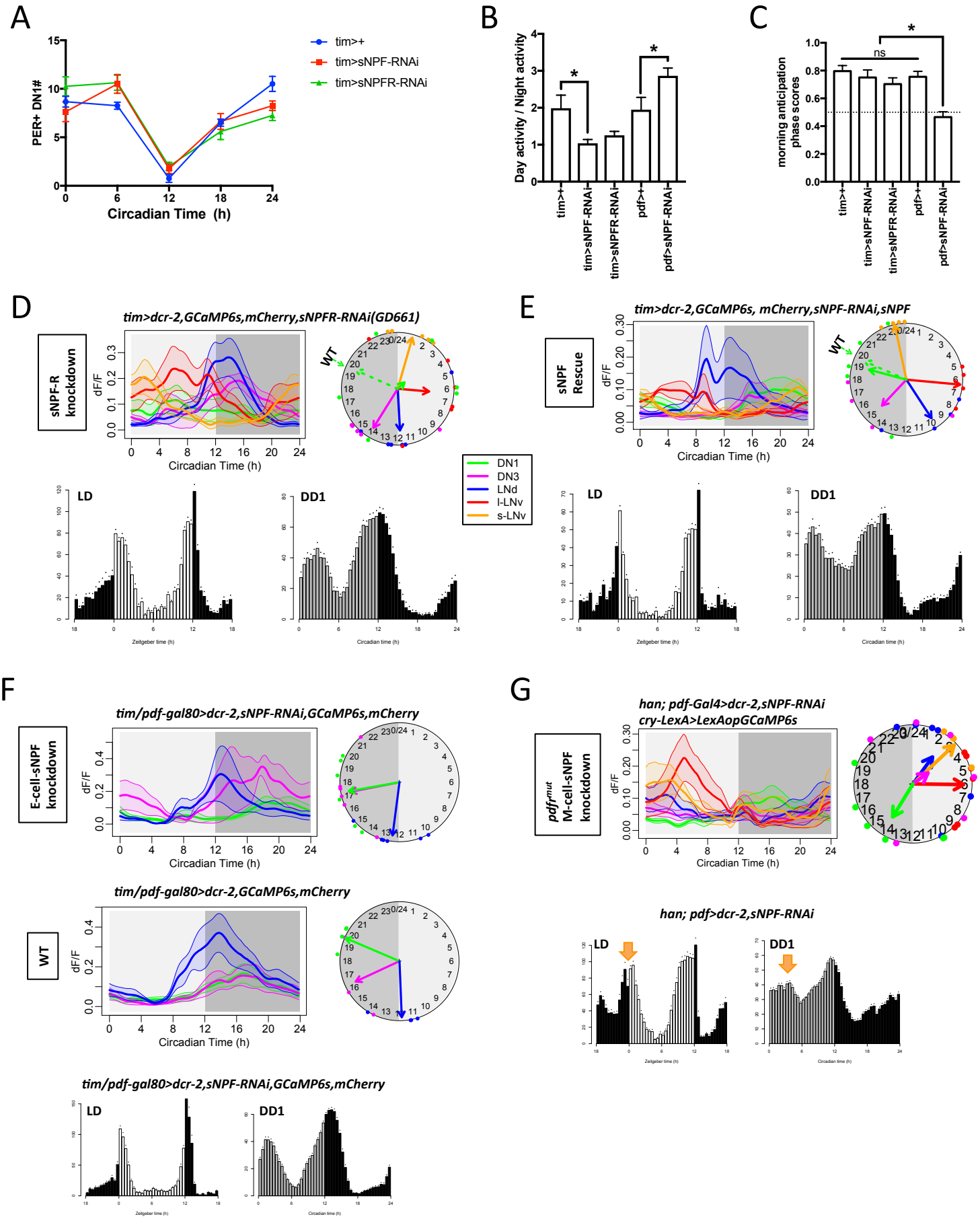

Figure S6. Additional characterization for the role of sNPF on regulating Ca^{2+} activity in DN1 pacemakers. Related to Figure 6.

(A) PER oscillations in DN1 groups were unaffected by sNPF/sNPFR knockdown. Quantifications of PER immunostaining brains from WT controls, pan-pacemaker RNAi knockdown of *sNPF*, and pan-pacemaker RNAi knockdown of *sNPFR* flies in first day under DD. PER(+) DN1 neurons were counted in each hemisphere. Error bars denote SEM (n = 6-10 hemispheres per time point). No significant differences were noted between genotypes.

(B) All-pacemaker sNPF knockdown decreases daytime locomotor activity and increases nighttime locomotor activity. M pacemaker sNPF knockdown increases daytime activity and decreases night activity. The amount of locomotor activity during the daytime or nighttime represents averages during a 6-day period under LD (*p<0.05; Mann-Whitney test). These results confirm previous work by Hermann-Luibl et al. (2014).

(C) M pacemaker sNPF knockdown impairs morning anticipatory behavior. Morning anticipation phase scores in different genotypes of control and sNPF knockdown flies (*p<0.01; ns, not significant: ANOVA followed by t-test). Scores below the dashed line indicate no anticipation.

(D) Above - Daily Ca^{2+} activity patterns in flies with sNPF receptor knockdown in all circadian pacemakers under DD (n = 6 flies), and their daily behavioral patterns under LD (below left) and DD (below right) conditions. WT refers to the peak value of the DN1 Ca^{2+} pattern in control flies.

(E) Above - Daily patterns in *tim* > *sNPF RNAi*, *sNPF* demonstrating full genetic rescue of the coherence and phase of DN1 Ca^{2+} activity under DD (n = 5 flies), and their daily behavioral patterns under LD (below left) and DD (below right) conditions.

(F) Daily Ca^{2+} activity and behavioral patterns of E-cell-specific sNPF knockdown flies. Average 24 hr Ca^{2+} transients (left) and Ca^{2+} phase distributions (right) under DD of three circadian pacemaker groups: the E-cell LNd group, the DN3, and DN1. Driven by *tim*-gal4/*pdf*-gal80, these three groups expressed both the Ca^{2+} sensor and *sNPF*-RNAi (above - n = 6 flies) and only the Ca^{2+} sensor as WT controls (middle - n = 5 flies). DN1 Ca^{2+} activity was rhythmic (p<0.01: Rayleigh test) and displayed a non-significant trend of phase-advance in E-cell-specific sNPF knockdown (p=0.058: Watson-Williams test). (Below) Average locomotor activity under LD cycles (below left) and in first day under DD (below right) in flies with *sNPF* knockdown in E pacemakers, *tim*-gal4, *pdf-gal80* > *sNPF RNAi.*

(G) Morning anticipatory behavior of *pdfr* mutants is restored by M-cell-specific sNPF knockdown. (Above) Average Ca^{2+} transients (left) and Ca^{2+} phase distributions (right) five major pacemaker groups in $pdfr^{han5304}$*;pdf > sNPF-RNAi* flies in the first day under DD (n = 6 flies). (Below) Average locomotor activity of $pdfr^{han5304}$*;pdf > sNPF-RNAi* flies under LD cycles (below left) and in first day under DD (below right); also see Table S1). In LD, these flies displayed strong morning anticipatory behavior (orange arrow), which is normally absent in *pdfr* mutants (Figure S2A) and in M-cell-specific sNPF knockdown flies (cf. Figure 6H). Note that the phase-advance of evening activity period in LD is not rescued.

Fig S7. Related to Figure 6

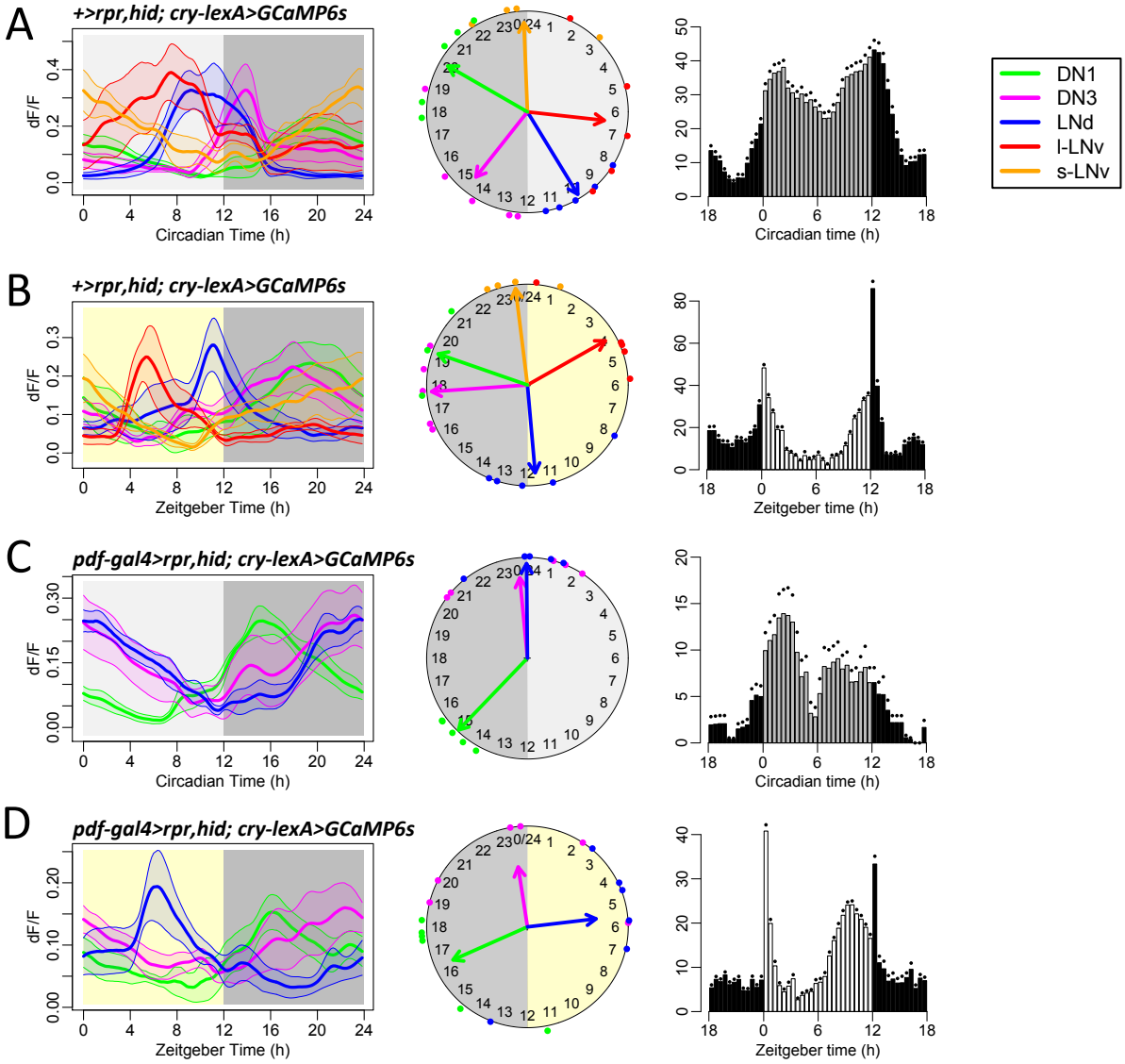

Figure S7. Daily Ca^{2+} activities and behavioral patterns of PDF-cell-ablated flies. Related to Figure 6. (A-B) Average Ca^{2+} transients (left), Ca^{2+} phase distributions (middle) and average locomotor activity (right) in WT (no Gal4) controls (A) in the first day under DD (n = 5 flies) and (B) under LD cycles (n = 5 flies).

(C-D) The Ca^{2+} activity patterns of three PDF-negative pacemaker groups in flies without PDF-positive neurons (s-LNv and l-LNv), and behavioral patterns of *pdf>rpr,hid*; *cry*>GCaMP6s flies. (C) In DD, compared to controls, LNd and DN3 were phase-shifted to dawn, while DN1 displayed a phase-advance ($p<0.01$: Watson-Williams test; n = 5 flies). (D) In LD, LNd phases were delayed, compared to values in DD, panel C) ($p<0.01$: Watson-Williams test; n = 6 flies); cf. Fig 1B.

Fig S8. Related to Figure 8

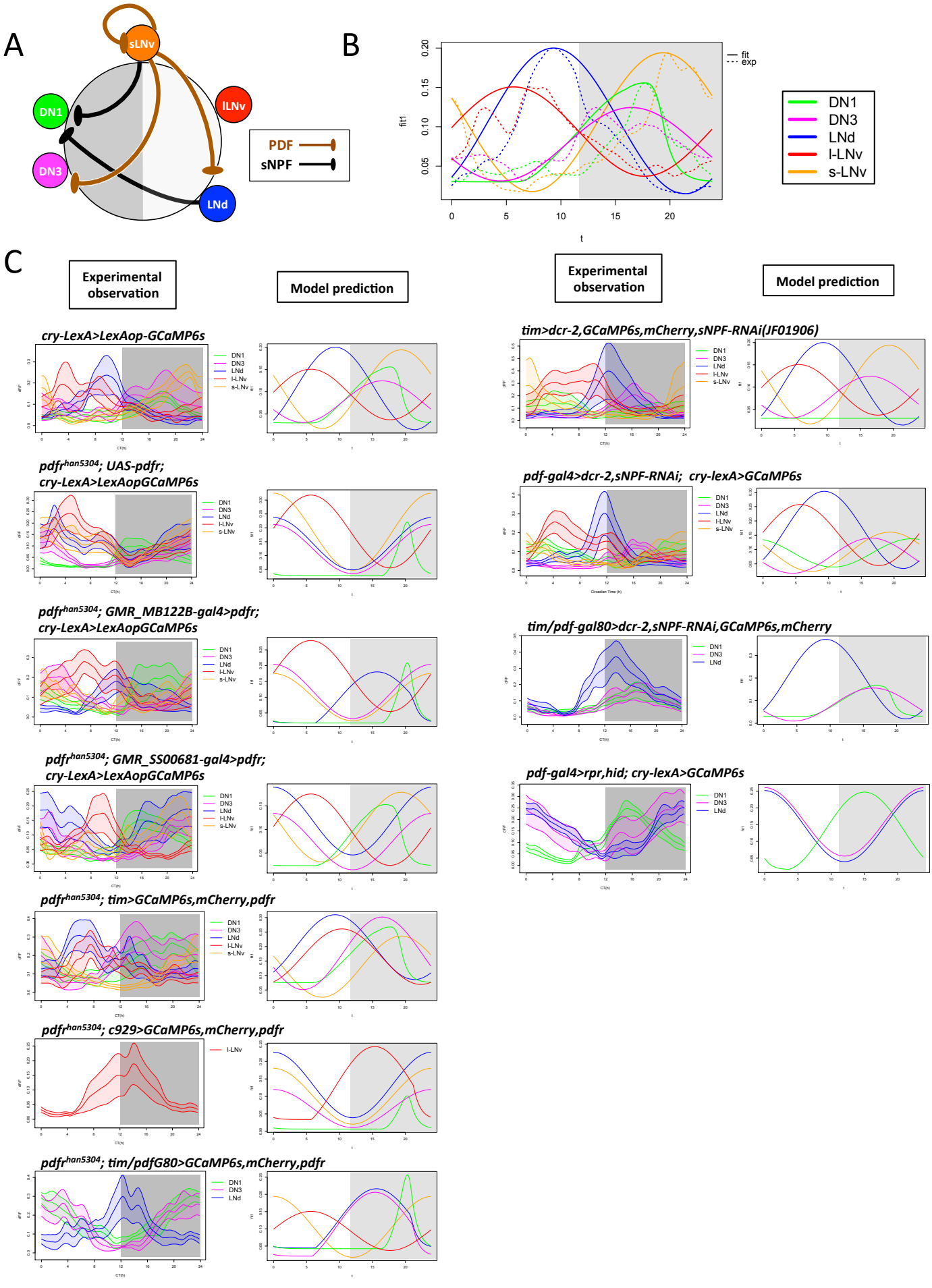

Figure S8. A quantitative model of oscillators coupled by PDF- and sNPF-mediated suppressions. Related to Figure 8.

(A) Schematics of the model: five simple harmonic oscillators represent Ca^{2+} rhythms of five major circadian pacemaker groups. These oscillators are coupled by PDF- and sNPF-mediated suppressions. (B) Ca^{2+} activity patterns of WT pacemakers (*cry*-lexA>*GCaMP6s* - dashed lines) were used to fit the model (solid lines). (C) Predictions of the model to removing or to adding neuropeptide-mediated interactions (right) were compared with the experimental observations (left – these are reproduced from earlier Figures).

Table S1. Summary of Circadian Behavior Rhythms. Related to Figure 1, 2, 4, and 6 and Figure S1, S2, S5, S6, and S7.

Genotype	N	%AR	Period	pwr	wid	SNR	ACT-day	ACT-night	ACT-cycle	E-phase* (ZT)	SEM
tim-gal4;uas-GCaMP6s,mCherry	16	44%	24.3	29.0	3.1	0.4	12.3	8.2	10.2	12.2	0.1
tim-gal4,uas-GCaMP6s;pdf01	14	79%	22.3	38.2	4.3	0.5	14.4	13.2	13.8	11.4	0.1
han/y;uas-pdfr/+; cryLexA,LexAop-GCaMP6s/+	16	56%	24.1	34.6	4.9	1.0	19.9	12.2	16.1	11.2	0.1
han/y;GMRSS00681/uas-pdfr;cryLexA,LexAop-GCaMP6s/+	15	53%	23.5	20.6	3.0	0.4	30.6	22.6	26.6	11.2	0.1
han/y;GMRMB122B/uas-pdfr; cryLexA,LexAop-GCaMP6s/+	8	63%	23.5	25.6	5.7	0.9	13.8	10.2	12.0	11.8	0.2
han/y;tim-gal4/ uas-pdfr;uas-GCaMP6s,mCherry/+	11	36%	23.6	44.8	4.0	1.6	19.2	26.2	22.7	12.6	0.4
han/y;pdfgal80/uas-pdfr;tim-gal4/uas-GCaMP6s,mCherry	12	50%	23.7	22.6	2.7	0.7	3.9	4.5	4.2	11.6	0.7
han/y;pdf-gal80/uas-pdfr;pdfr(B)-gal4/uas-GCaMP6s,mCherry	15	40%	23.8	19.1	2.5	0.4	7.7	8.7	8.2	11.2	0.2
han/y;c929-gal4/uas-pdfr; uas-GCaMP6s,mCherry/+	10	70%	23.7	6.3	1.3	0.6	12.7	10.1	11.4	11.8	0.1
pdf-gal4/uas-pdfr; GCaMP6s,mCherry/+	14	43%	24.5	37.2	4.4	0.5	15.4	12.2	13.8	12.0	0.3
DH31[01];timgal4/uas-GCaMP6s	15	7%	24.7	37.9	4.4	0.7	7.4	5.5	6.5	12.1	0.1
dcr2/y;timgal4/+;GCaMP6s,mCherry/CG17415(JF01945)-RNAi	15	20%	24.3	39.2	5.3	0.6	20.1	10.1	15.1	11.5	0.2
dcr2/y;timgal4/+;GCaMP6s,mCherry/ GC4395(GD724)-RNAi	15	0%	23.5	70.8	7.9	2.4	34.3	22.1	28.2	12.8	0.2
dcr2/y;timgal4/ITP(JF01817)-RNAi; GCaMP6s,mCherry/+	7	0%	23.6	39.2	4.3	1.4	30.5	15.7	23.1	12.2	0.1
dcr2/y;timgal4/+;GCaMP6s,mCherry/ NPF(JF02555)-RNAi	16	6%	24.1	46.6	5.8	1.3	23.0	9.6	16.3	11.6	0.1
dcr2/y;tim-gal4/+;GCaMP6s,mCherry/ NPFR(KK112704)-RNAi	14	36%	25.2	22.6	4.1	0.6	15.9	12.6	14.2	11.9	0.1

Genotype	N	%AR	Period	pwr	wid	SNR	ACT-day	ACT-night	ACT-cycle	E-phase(ZT)	SEM
dcr2/y;tim-gal4/+; GCaMP6s,mCherry/ sNPF(JF01906)-RNAi	15	0%	23.9	37.0	4.4	1.1	31.6	23.4	27.5	12.0	0.1
pdf-gal4/y;;cry-LexA,LexAop-GCaMP6s	15	27%	23.7	59.4	4.0	0.5	18.4	11.5	14.9	12.1	0.2
pdf-gal4/y;uas-dcr2/+;cry-LexA,LexAop-GCaMP6s/uas-sNPF(JF01906)-RNAi	32	19%	23.6	24.4	3.0	0.5	18.1	8.9	13.4	10.0	0.2
dcr2/y;tim-gal4/+;GCaMP6s,mCherry/ sNPFR(GD661)-RNAi	22	9%	23.9	55.3	6.8	1.7	36.6	19.8	28.2	11.9	0.2
dcr2/y;tim-gal4/ sNPF;GCaMP6s,mCherry /+	7	29%	24.5	51.4	4.6	0.7	28.8	16.6	22.7	11.7	0.2
dcr2/y;tim-gal4/ sNPF;GCaMP6s,mCherry / sNPF(JF01906)-RNAi	8	25%	24.3	55.9	4.6	0.6	23.9	13.9	18.9	11.6	0.1
han,pdf-gal4/y;uas-dcr2/+;uas-sNPF(JF01906)-RNAi/+	28	57%	23.4	16.9	2.7	0.4	43.1	30.8	36.9	11.4	0.1
uas-dcr2/pdf-gal80;tim-gal4,uas-GCaMP6s/uas-sNPF(JF01906)-RNAi	16	19%	23.6	66.0	3.8	0.9	17.4	8.9	13.1	12.1	0.1
uas-rpr/y;;cry-LexA,LexAop-GCaMP6s	14	7%	23.8	64.3	4.2	0.8	23.1	11.1	17.1	12.4	0.2
uas-rpr,hid;pdf-gal4;cry-LexA,LexAop-GCaMP6s	12	100%	NA	4.8	1.0	0.5	7.0	7.5	7.2	10.1	0.2

* E-phases and SEM are calculated from behavior in LD cycles. The E-phases are given in Zeitgeber time (ZT), in which the average evening peak fell; SEM represents fly-to-fly variability within a given genotype. The rest of values are calculated from nine-day records of behaviour in DD.